

Synthesis and Characterization of a Brønsted Pair Functionalized Shape-Persistent Macrocycle

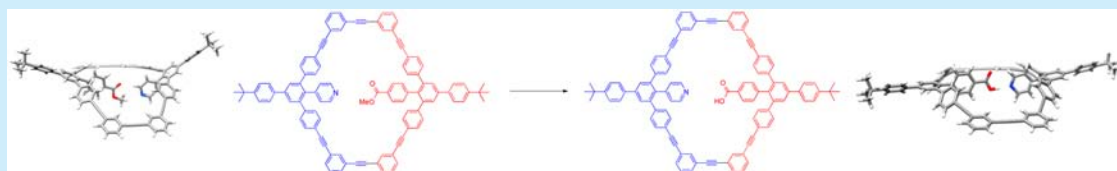
Annette B. Vliegthart,[†] Frank A. L. Welling,[†] Michael Roemelt,^{*,‡,§} Robertus J. M. Klein Gebbink,[†] and Matthias Otte^{*,†}

[†]Organic Chemistry & Catalysis, Debye Institute for Nanomaterials Science, Universiteit Utrecht, Universiteitsweg 99, 3584 CG Utrecht, The Netherlands

[‡]Lehrstuhl für Theoretische Chemie, Ruhr-Universität Bochum, D-44780 Bochum, Germany

[§]Max-Planck Institut für Kohlenforschung, Kaiser-Wilhelm-Platz 1, D-45470 Mülheim an der Ruhr, Germany

S Supporting Information



ABSTRACT: The first shape-persistent macrocycle **1** offering a Brønsted pair functionalized interior is described. Via postcyclization transformation, this heterosequenced compound can be obtained from its corresponding ester **2**. The macrocycles differ dramatically in their characteristics such as solubility and appearance. Theoretical investigations suggest that those contrasts might originate from conformational changes due to the formation of a strong O–H–N hydrogen bond in **1**.

The design of complex and well-defined, purely organic architectures is a vital field in modern chemistry. Thereby structures of different dimensions such as macrocycles,¹ cages,² and periodical covalent organic frameworks have been developed.³ Some of the structures have been found to be suitable materials for gas storage,⁴ as receptors,⁵ or as catalysts.⁶ Among them, shape-persistent macrocycles consisting of fully π -conjugated backbones are a fascinating class of compounds. Examples are cyclic phenylene macrocycles,⁷ phenylene–ethynylene macrocycles,⁸ heterocycle–ethynylene macrocycles,⁹ and mixed phenylene–heterocycle–ethynylene macrocycles.¹⁰ In particular, their assembly on surfaces,¹⁰ their photophysical properties,¹¹ and host abilities have been studied.¹² Most reported shape-persistent macrocycles are highly symmetrical compounds that are often synthesized via homocouplings.¹ As a consequence, their interior, which significantly determines their characteristics, is also symmetrical. The design of heterosequenced interiors may lead to new applications as organocatalysts, *trans*-ligands for transition metals or the selective encapsulation of polar guest compounds. To date, examples of shape-persistent macrocycles offering a heterosequenced, less symmetrical interior are rare.^{10,13} In this regard also, only a limited scope of functional groups have yet been employed in such heterosequenced interiors. In particular, an opposing functionalized interior is of high interest, as it might offer new opportunities in encapsulation chemistry and catalysis.

Within the work presented here, we pursue the synthesis of the conceptually new heterosequenced shape-persistent macrocycle **1** (Scheme 1). Compound **1** offers a bifunctionalized interior that consists of a Brønsted pair, namely, a carboxylic acid and a

pyridine base moiety. To our knowledge Brønsted pair functionalized interiors are unprecedented for shape-persistent macrocycles.

We envisioned that **1** could be obtained via a postcyclization transformation from ester-functionalized macrocycle **2** (Scheme 1). Terminal dialkyne **3** and diiodide **4** seemed to be promising substrates for a macrocyclization via a Sonogashira reaction. As macrocycles **1** and **2** contain mainly arylene and ethynylene units, self-aggregation via π -stacking might occur.¹⁴ Other self-aggregated shape-persistent macrocycles have shown to be heterogeneous catalysts.¹⁵

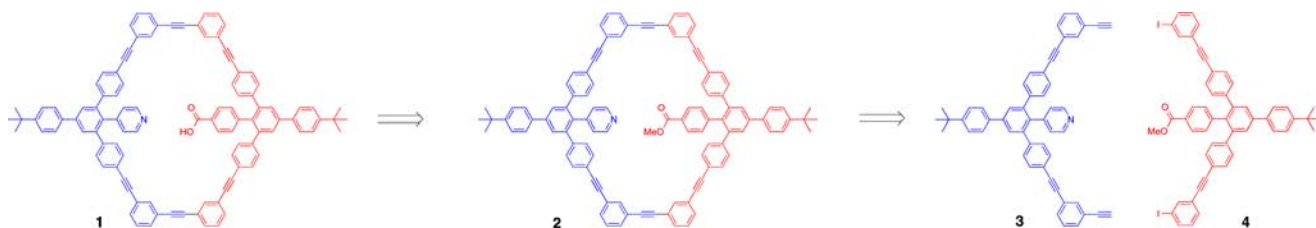
The synthesis of building blocks **3** and **4** is depicted in Scheme 2. Compounds **5**, **6**, and **7** have been synthesized similar to a protocol described by Höger.⁸ From **6** and **7**, macrocycle precursors **3** and **4** are obtained via common Sonogashira reaction and deprotection strategies.

With **3** and **4** in hand the macrocyclization toward the ester and pyridine functionalized compound **2** via Sonogashira reaction was explored. An initial experiment was carried out at 40 °C using triethylamine (substrate concentration 0.01 M) as the solvent. Unfortunately, **4** is badly soluble in triethylamine, which resulted in a complicated product mixture and ca. 50% recovered **4**. In a second attempt, a NEt₃/THF 2:1 solvent mixture was used. In this case, product formation was observed, while the yield was rather low (10%). We concluded that slow addition of a THF solution of **3** and **4** (0.15 mmol solved in 15 mL THF) to a solution of catalysts in NEt₃ (20 mL) might

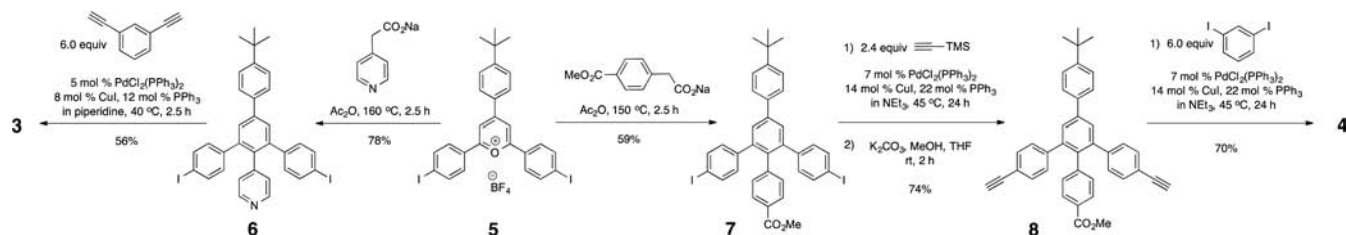
Received: July 6, 2015

Published: August 25, 2015

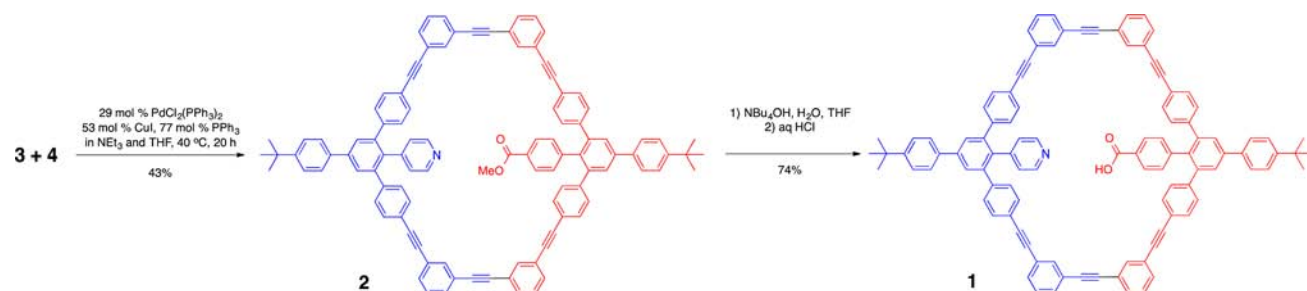
Scheme 1. Retrosynthetic Analysis of the Shape-Persistent Heterosequenced Macrocycle 1



Scheme 2. Synthesis of Building Blocks 3 and 4



Scheme 3. Synthesis of the Brønsted Pair Functionalized Macrocycle 1 via 2



improve the yield. After filtration of insoluble reaction products (probably oligomers), extraction with CH_2Cl_2 and purifying by column chromatography (eluent CHCl_3), **2** could be isolated in 28% yield. Further optimization on the addition rate and a higher THF/ NEt_3 ratio prevented formation of insoluble byproducts and gave **2** in a good yield of 43% (Scheme 3).

Macrocycle **2** has been characterized via high resolution ESI-MS, elemental analysis, ^1H NMR, ^{13}C NMR, DOSY, H_2H -COSY, and IR spectroscopy. The ESI-MS analysis indicated the formation of **2** by showing a signal at $m/z = 1380.5781$, which corresponds to $[\mathbf{2} + \text{H}^+]$ (theoretical value $m/z = 1380.5719$). No signals with higher m/z values have been detected. However, weak signals corresponding to a double charged species $[(\mathbf{2} + \text{H}^+)_2]$ were observed.

Figure 1 shows the ^1H NMR spectra of **3**, **4**, and **2** from 9.0 to 3.0 ppm (for full spectra see the Supporting Information). From the signals around 6.9 and 8.3 ppm in (a) and (c) it can be concluded that the pyridine moiety is present in **2** and **3**. The characteristic signals of the terminal alkynes around 3.2 ppm disappeared completely in Figure 1c. The signal in Figure 1b at around 7.9 ppm corresponds to the proton that is in *ortho*-position to the iodine and the alkyne in **4**. This signal has completely disappeared in Figure 1c. The spectrum of **2** shows a signal around 3.8 ppm that corresponds to the methyl ester moiety. The ^{13}C NMR spectrum of **2** shows six signals between 90 and 87 ppm corresponding to the three different internal alkynes (see Supporting Information). Overall, it can be concluded that **2** is pyridine and carbocyclic ester functionalized and contains three internal alkynes, while no terminal alkyne or aryl iodide functionalization is observed. Additional NMR

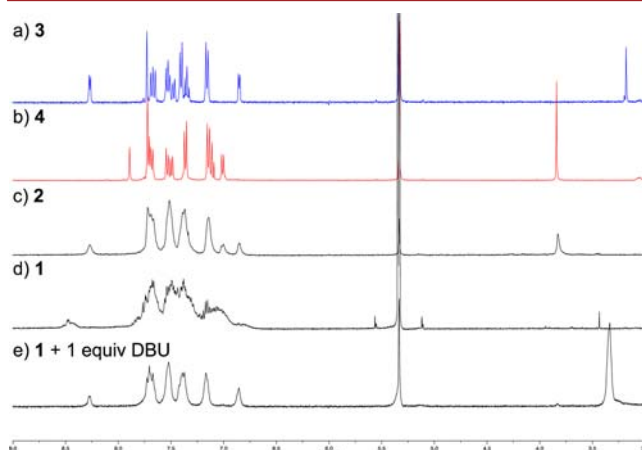


Figure 1. ^1H NMR spectra of (a) **3**, (b) **4**, (c) **2**, (d) **1**, and (e) **1** plus 1 equiv of DBU (1,8-diazabicyclo[5.4.0]undec-7-ene) (9.0–3.0 ppm). Spectra were recorded in CD_2Cl_2 at 25 $^\circ\text{C}$.

analysis using DOSY and H_2H -COSY techniques further confirm the successful synthesis and isolation of **2** (see Supporting Information).

Notably, the signals in Figure 1c are relatively undefined and broad. The protons in **2** should show up as 25 different signals that are often overlapping while showing different multiplicity. It is known that such macrocycles can adapt different conformations that may lead to more complicated ^1H NMR spectra.¹⁶ In addition, it has been shown for related systems that broad signals can be caused by hindered rotations within the macrocyclic

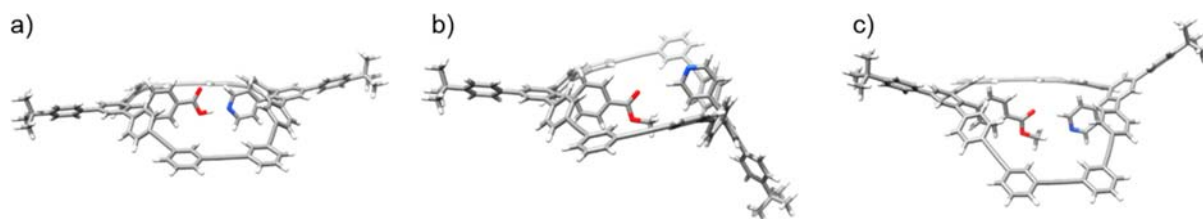


Figure 2. Preferred conformations of **1** (a) and **2** (b,c) as obtained from DFT geometry optimizations. In the case of compound **2**, two stable conformers with chair-like (b) and boat-like (c) structures were obtained.

structures.¹⁶ Indeed, when **2** is measured in deuterated 1,2-dichlorobenzene at 95 °C, signals of the para-substituted phenylrings belonging to the macrocyclic core are more defined (see [Supporting Information](#)). Broad signals could also be the result of π -stacking phenomena.¹⁷ This is supported by three observations. Clear CD₂Cl₂ solutions of **2** form an ordered and insoluble precipitate during longer NMR measurements. In addition, ESI-MS shows weak signals of dimeric [(**2** + H⁺)₂]. Finally, when a dichloromethane solution of **2** is evaporated, **2** is obtained in one piece that has the appearance of a yellowish thin foil (see [Supporting Information](#)).

With **2** in hand we investigated its potential for a postcyclization manipulation to obtain macrocycle **1** that offers a Brønsted pair functionalized interior. Unfortunately, an initial approach of basic hydrolysis using aq. NaOH in THF failed. However, employing aqueous tetrabutylammoniumhydroxide in THF followed by an acidic workup result in the formation of **1** in 74% yield ([Scheme 3](#)). Compound **1** has been characterized by ¹H NMR, elemental analysis, IR and ESI-MS measurements. It is poorly soluble in chlorinated solvents and insoluble in all other solvents tested (e.g., toluene, cyclohexane, THF, ether, methanol). Nevertheless we were able to record a ¹H NMR spectrum of **1** in CD₂Cl₂, which shows no methyl ester signal at 3.8 ppm anymore ([Figure 1d](#)); for full spectrum see [Supporting Information](#)). Instead traces of methanol were observed. The pyridine signals became even broader while also showing a discrete doublet; this may indicate a partial protonation of the pyridine nitrogen in solution. Comparing the IR spectra of **2** and **1** shows a small shift of the absorption in the carbonyl region from 1720 to 1715 cm⁻¹. This can be a further indication for the successful carboxylic acid formation. However, the IR spectra do not indicate a protonation of the pyridine moiety in the solid state. To our delight the ESI-MS showed a signal at *m/z* = 1366.5596 that corresponds to [**1** + H⁺] (theoretical value *m/z* = 1366.5563). Beside this the only signal that is observed above *m/z* = 300 corresponds to **2** and the dimeric forms [(**1** + H⁺)₂] and [(**2** + H⁺)₂]. Samples of **1** contain only traces of **2** that may be easier ionized than **1** as the ¹H NMR of **1** shows clearly no methyl ester signals. Elemental analysis provides further evidence that **1** has been successfully synthesized as the measured and calculated values for carbon, hydrogen, and nitrogen match nicely (measured, C = 91.23%, H = 5.31%, N = 0.95%; calculated, C = 91.40%, H = 5.24%, N = 1.02%). All attempts to obtain crystals suitable for X-ray diffraction analysis resulted in the formation of amorphous solids. To the best of our knowledge, **1** is the first opposing functionalized shape-persistent macrocycle that offers a Brønsted pair functionalized interior.

In order to obtain insight into the preferred conformations of **1** and **2**, DFT calculations were carried out with the ORCA program package.¹⁸ The geometries of **1** and **2** were optimized using a computational setup that yielded accurate results in a large set of benchmark calculations on organic molecules (see

[Supporting Information](#)).¹⁹ As depicted in [Figure 2a](#) the carboxylic acid and the pyridine in the interior of **1** form a stable (see below) adduct. The key feature of this adduct is an almost perfectly linear O–H–N hydrogen bond ($\angle(\text{OHN}) = 178.9^\circ$) with an O–H distance of 1.03 Å and a N–H distance of 1.67 Å. Such a N–H interaction could explain the observed broadened pyridine signal in the ¹H NMR spectrum of **1**. In order to provide the linear alignment of the two functional groups, the arm that bears the pyridine is tilted out of the molecular plane. As a consequence the entire ring structure of **1** takes a slightly arched form ([Figure 2a](#)). However, since the curvature is small the structure of **1** should still allow for parallel assembly of multiple molecules chaperoned by π -stacking effects. Moreover, we would like to note that the ring experiences a minor ring strain reflected in alkyne bond angles between 176.5° and 178.0°.

The strength of the O–H–N hydrogen bond was estimated by optimizing a second, metastable conformer where the two functional groups do not form a hydrogen bond (see [Supporting Information](#)). The energy difference between the two conformers is calculated to be 30.9 kcal/mol. Although the energy difference depends on all geometric changes between the two conformers, we assume that a large fraction of it can be attributed to breaking the strong hydrogen bond between the carboxylic acid and the pyridine. In contrast to the observations made for **1** no hydrogen bond can be formed between the pyridine and the ester in **2**. Owing to this lack of a bonding interaction and the increased steric demand of the methyl group, the two arms of **2** undergo a rather strong tilting movement out of the molecular plane ([Figure 2b,c](#)). Two stable conformers could be optimized with the two functional groups located on the same side or on opposite sides of the ring resulting in a boat-like or chair-like structure, respectively ([Figure 2b,c](#)). According to our DFT calculations, the boat-like structure is by 4.4 kcal/mol more stable. A relaxed surface scan indicates that the barrier for the interconversion between both conformers is on the order of ~3 kcal/mol (see [Supporting Information](#)). The lack of a strong O–H–N hydrogen bond and the concomitant increased accessibility of the functional groups of **2** might be the cause for its different solubility and macroscopic appearance as compared to **1**.

To investigate the bifunctional nature of **1**, its behavior toward DBU (1,8-diazabicyclo[5.4.0]undec-7-ene) as a strong base and trifluoroacetic acid as a strong acid has been studied. Upon addition of 1 equiv of DBU to **1**, its ¹H NMR spectrum changes dramatically (see [Figure 1e](#)). The spectrum depicted in [Figure 1e](#) looks similar to that of **2** ([Figure 1c](#)). Comparing those, it appears that the signal at 7.0 ppm in [Figure 1c](#), which corresponds to the protons next to the carboxylic ester group, has shifted in [Figure 1e](#) and overlaps with the pyridine signal at 6.8 ppm. Furthermore, due to addition of base, the solubility of **1** increases. The addition of trifluoroacetic acid also results in a more defined ¹H NMR

spectrum (see Supporting Information). However, while base addition influenced the shifts of protons next to the carboxylic acid moiety, addition of acid does not result in significant shifts. A DFT optimization of $1+H^+$ confirms that it structurally resembles **1** as it features a N–H–O hydrogen bond and almost perfectly linearly arranged arms (see Supporting Information). In contrast to the above described hydrogen bond in **1**, the hydrogen in $1+H^+$ is located closer to the pyridine moiety than to the carboxylic oxygen ($d(N-H) = 1.05 \text{ \AA}$ and $d(O-H) = 1.68 \text{ \AA}$). This arrangement thus corresponds to a protonated pyridine that is stabilized by the carboxyl group. The arms of $1-H^+$, however, are strongly tilted, similar to those of **2**, which could explain the similarity between the spectra in Figure 1c,e.

In conclusion, we synthesized shape-persistent macrocycle **2**, which can be transformed into macrocycle **1**. This offers a new and unsymmetrical functionalized Brønsted pair interior that to our knowledge is unprecedented. Computational investigations revealed that **1** features a strong interaction between the carboxylic acid and the pyridine enforcing an almost planar structure. Addition of base disturbs this interaction while leading to conformational changes. We believe that conceptually new opposing functionalized shape-persistent systems such as the presented ones can play an important role in material science, supramolecular chemistry, and catalysis.

■ ASSOCIATED CONTENT

📄 Supporting Information

The Supporting Information is available free of charge on the ACS Publications website at DOI: [10.1021/acs.orglett.5b01931](https://doi.org/10.1021/acs.orglett.5b01931).

Experimental procedures, spectral data, computational data, and other characterization data (PDF)

■ AUTHOR INFORMATION

Corresponding Authors

*(M.O.) E-mail: m.otte@uu.nl.

*(M.R.) E-mail: michael.roemelt@theochem.ruhr-uni-bochum.de.

Notes

The authors declare no competing financial interest.

■ ACKNOWLEDGMENTS

M.O. acknowledges the sustainability theme of Utrecht University for funding. M.R. would like to thank the Otto-Hahn Award program of the Max Planck society for funding.

■ REFERENCES

- (1) (a) Zhang, W.; Moore. *Angew. Chem., Int. Ed.* **2006**, *45*, 4416. (b) Iyoda, M.; Yamakawa, J.; Rahman, M. J. *Angew. Chem., Int. Ed.* **2011**, *50*, 10522.
- (2) (a) Zhang, G.; Mastalerz, M. *Chem. Soc. Rev.* **2014**, *43*, 1934. (b) Zhang, G.; Presly, O.; White, F.; Opper, I. M.; Mastalerz, M. *Angew. Chem., Int. Ed.* **2014**, *53*, 5126. (c) Wang, Q.; Yu, C.; Long, H.; Du, Y.; Jon, Y.; Zhang, W. *Angew. Chem., Int. Ed.* **2015**, *54*, 7550.
- (3) Feng, X.; Ding, X.; Jiang, D. *Chem. Soc. Rev.* **2012**, *41*, 6010.
- (4) Huang, N.; Krishna, R.; Jiang, D. *J. Am. Chem. Soc.* **2015**, *137*, 7079.
- (5) Ke, C.; Destecroix, H.; Crump, M. P.; Davies, A. P. *Nat. Chem.* **2012**, *4*, 718.
- (6) Zhang, Q.; Tiefenbacher, K. *Nat. Chem.* **2015**, *7*, 197.
- (7) Hensel, V.; Schlüter, A. D. *Chem. - Eur. J.* **1999**, *5*, 421.
- (8) Klyatskaya, S.; Dingenouts, N.; Rosenauer, C.; Müller, B.; Höger, S. *J. Am. Chem. Soc.* **2006**, *128*, 3150.

(9) Tobe, Y.; Nagano, A.; Kawabata, K.; Sonoda, M.; Naemura, K. *Org. Lett.* **2000**, *2*, 3265.

(10) Grave, C.; Lentz, D.; Schäfer, A.; Samori, P.; Rabe, J. P.; Franke, P.; Schlüter, A. D. *J. Am. Chem. Soc.* **2003**, *125*, 6907.

(11) Mössinger, D.; Chaudhuri, D.; Kudernac, T.; Lei, S.; De Feyter, S.; Lupton, J. M.; Höger, S. *J. Am. Chem. Soc.* **2010**, *132*, 1410.

(12) (a) Castro-Fernández, S.; Lahoz, I. R.; Llamas-Saiz, A. L.; Alonso-Gómez, J. L.; Cid, M.-M.; Navarro-Vázquez, A. *Org. Lett.* **2014**, *16*, 1136.

(b) Popov, I.; Chen, T.-H.; Belyakov, S.; Daugulis, O.; Wheeler, S. E.; Miljanic, O. Š. *Chem. - Eur. J.* **2015**, *21*, 2750.

(13) (a) Höger, S.; Meckenstock, A.-D. *Chem. - Eur. J.* **1999**, *5*, 1686.

(b) Hartley, C. S.; Moore, J. S. *J. Am. Chem. Soc.* **2007**, *129*, 11682.

(c) Yamasaki, R.; Shieto, A.; Saito, S. *J. Org. Chem.* **2011**, *76*, 10299.

(d) Okochi, K. D.; Jin, Y.; Zhang, W. *Chem. Commun.* **2013**, *49*, 4418.

(e) Okochi, K. D.; Han, G. S.; Aldridge, I. M.; Liu, Y.; Zhang, W. *Org. Lett.* **2013**, *15*, 4296.

(14) Shetty, A. S.; Zhang, J.; Moore, J. S. *J. Am. Chem. Soc.* **1996**, *118*, 1019.

(15) Dawn, S.; Salpage, S. R.; Koscher, B. A.; Bick, A.; Wibowo, A. C.; Pellechia, P. J.; Shimizu, L. S. *J. Phys. Chem. A* **2014**, *118*, 10563.

(16) Höger, S.; Bonrad, K.; Mourran, A.; Beginn, U.; Müller, M. *J. Am. Chem. Soc.* **2001**, *123*, 5651.

(17) Lei, S.; Heyen, A. V.; De Feyter, S.; Surin, M.; Lazzaroni, R.; Rosenfeldt, S.; Ballauff, M.; Lindner, P.; Mössinger, D.; Höger, S. *Chem. - Eur. J.* **2009**, *15*, 2518.

(18) Neese, F. *Wiley Interdisciplinary Reviews: Computational Molecular Science* **2012**, *2*, 73.

(19) Goerigk, L.; Grimme, S. *Phys. Chem. Chem. Phys.* **2011**, *13*, 6670.